Effect of $CaCO_3$ on the Wood Properties of Tropical Hardwood Species from Fast-growth Plantation in Costa Rica

Roger Moya,[a,*] Johanna Gaitán-Álvarez,[a] Alexander Berrocal,[a] and Fabio Araya [b]

This work aimed to evaluate the effect of the precipitation of $CaCO_3$ *via* subsequential *in-situ* mineral formation based on a solution-exchange process of two solution-exchange cycles *via* impregnation with $CaCl_2$ in ethanol and $NaHCO_3$ in water. The effects were investigated in terms of the structure of the wood and the thermal, physical, mechanical, and decay resistance properties of nine species commonly used in commercial reforestation in Costa Rica. The thermogravimetric analysis results showed that the woods with the highest formation of $CaCO_3$ showed a more pronounced signal at 200 °C in relation to untreated/wood; therefore, they were more thermostable. The fire-retardancy test showed that flame time in $CaCO_3$/wood composites was longer than for untreated/wood in half of the species tested, presenting a positive effect of mineralization. Wood density, decay resistance, modulus of rupture (MOR), modulus of elasticity (MOE) in flexion, and MOR in compression were slightly affected by mineralization. Water absorption increased, but it had no negative effect on the dimensional stability. In general, mineralization can be a chemical treatment to increase the dimensional stability and fire resistance of hardwood species without modifying the wood's physical and mechanical properties.

Keywords: Wood treatment; Wood chemical treatment; Wood plantation; Fast-growth plantation; Wood properties

*Contact information: a: Instituto Tecnológico de Costa Rica, Escuela de Ingeniería Forestal, Apartado 159-7050, Cartago, Costa Rica; b: Centro de Investigación y de Servicios Químicos y Microbiológicos (CEQIATEC), Escuela de Química, Instituto Tecnológico de Costa Rica, Cartago 159-7050, Costa Rica; * Corresponding author: rmoya@itcr.ac.cr*

INTRODUCTION

Minerals are common in living organisms, where they maintain rigidity and hardness of the structures. The process of mineral formation by living organisms is known as biomineralization (Krajewska 2018). Minerals are also found in different shapes and sizes in natural deposits in the Earth's crust (Krajewska 2018). Biomineralization can be biologically controlled in the cell process (Benzerara *et al.* 2011; Gadd *et al.* 2012, 2014; Li *et al.* 2014, 2015; Kumari *et al.* 2016). There are around 60 different biological minerals (Anbu *et al.* 2016). The Earth's crust minerals constitute over 4% of biological minerals, and they are commonly found in rocks such as chalk, marble, travertine, and tuff, among others (Krajewska 2018).

Among the wide range of minerals from biomineralization and deposits of the Earth's crust, calcium carbonate ($CaCO_3$) is the main product and is considered the most useful today (Rodriguez-Navarro *et al.* 2012; Dhami *et al.* 2013; Kumari *et al.* 2016). Additionally, $CaCO_3$ appears as different polymorphs (calcite, aragonite, and vaterite); two hydrated polymorphs (monohydrocalcite and ikaite), and several amorphous phases (Sáãnchez-Román *et al.* 2007; Dhami *et al.* 2014). Calcite is the primary $CaCO_3$ product and it is the most thermodynamically stable polymorph of $CaCO_3$ (Okwadha and Li 2010; Ganendra *et al*. 2014). Vaterite, in turn, is considered a minor, metastable and transitional phase to calcite formation (Tourney and Ngwenya 2009). This mineral has been used for decades in construction and, more recently, it has been implemented in the agricultural, medical and engineering industries (Hoque 2013). Specifically, it is applied in the paper, paint, food, ceramics, construction, ink, adhesives, drugs, cable, and plastic industries (Ozen *et al.* 2013). In the plastics industry for example, it is used as a loading agent to substitute high value polymers (Ozen *et al.* 2013). For water purification it can be used to eliminate ions of heavy metals such as Cu^{+2}, Pb^{+2}, Cd^{+2}, Zn^{+2}, and Cr^{+5} (Hong *et al*. 2011). In the paper industry, it is used for producing high gloss, greater opacity and whiteness (Barhoum *et al.* 2014; Wu *et al.* 2016).

In contrast, wood has a porous network that poses a series of limitations, namely, high moisture content and hygroscopicity, dimensional instability, and high flammability (Uribe and Ayala 2015). However, this porous network is an optimal platform for the deposition of inorganic matter such as $CaCO_3$ (Merk *et al.* 2016); therefore, minerals can be introduced in its hierarchical structure to help improve the material characteristics (Tampieri *et al.* 2009; Hübert *et al.* 2010; Shabir Mahr *et al.* 2012). Nevertheless, the precipitation process of crystals of $CaCO_3$ is highly complex, because it depends on factors that affect the nucleation process and the subsequent crystal growth, which are often difficult to control (Declet *et al*. 2016).

Nevertheless, the first experiences on mineralization or $CaCO_3$ formation inside the wood were reported a few years ago (Tsioptsias and Panayiotou 2011; Merk *et al.* 2015; Uribe and Ayala 2015). Tsioptsias and Pahayictou (2011) introduced $CaCO_3$ using aqueous solutions and supercritical carbon dioxide in *Picea abies*, corroborating that under controlled conditions the treatment has fire-retardant effects. They concluded that the fire retardation is achieved in both glowing and smolding combustion and may be due to different mechanisms. Seeking fire retardancy, Merk *et al.* (2015, 2016) used a modern and simple method based on a subsequential *in-situ* mineral formation based on a solution-exchange process in beech and spruce woods. Those studies showed that the formation of crystals of polycrystalline calcite and vaterite inside the wood occurs in lumina vessels and to a lesser extent in adjacent cell walls. Recently, using the methodology proposed by Merk *et al.* (2016), Gaitán-Alvarez *et al.* (2020) studied $CaCO_3$ precipitation in tropical hardwoods and determined that it occurs in the form of calcite and vaterite, mainly in the vessels and rays of the species. They also determined that *in-situ* crystal formation is difficult to control.

Despite the mentioned studies, the knowledge about the effect of $CaCO_3$ precipitation on the wood properties is limited; besides, the studies are limited to a few softwoods, such as beech, spruce, and *Picea*, and the processes of wood impregnation have been performed at a low scale (Tsioptsias and Panayiotou 2011; Klaithong *et al.* 2013;

Burgert *et al.* 2016). Because of the great number of tropical timber species and the large variety of anatomical structures (Tenorio *et al.* 2016; Liu *et al.* 2018), studying the effect of $CaCO_3$ precipitation on wood properties becomes highly relevant to solve the problems of high moisture content, dimensional stability, and natural decay, among others (Mantanis 2017).

Given this context, the present work aimed at evaluating the effects of $CaCO_3$ precipitation on wood structure, on the thermal properties (thermal stability and fire retardancy), physical properties (density, moisture content, water absorption by immersion, swelling, and moisture equilibrium), mechanical properties (static flexure and grain parallel compression), and durability properties (natural decay) of nine species commonly used in commercial reforestation in Costa Rica. Studying these effects, it will be possible to treat tropical species with $CaCO_3$ to increase their fire retardancy and characterize the principal changes in wood properties.

EXPERIMENTAL

Materials

Sapwood from nine species from fast growth forest plantations in Costa Rica presenting good permeability was used (Moya *et al.* 2015). The species were *Cedrela odorata* (*Co*), *Cordia alliodora* (*Ca*), *Enterolobium cyclocarpum* (*Ec*), *Gmelina arborea* (*Ga*), *Hieronyma alchorneoides* (*Ha*), *Samanea saman* (*Ss*), *Tectona grandis* (*Tg*), *Vochysia ferruginea* (*Vf*), and *Vochysia guatemalensis* (*Vg*). The age of the plantations that contributed the material ranged between 4 and 8 years. Three trees per species were cut down for sampling. Then, the samples were cut into 1-m-long logs and sawn into 7.5 cm wide × 2.5-cm-thick boards. These boards were air dried until 12 to 15% moisture content was reached. Then, pieces 46 cm (length) × 7.5 cm (width) × 2 cm (thickness) were extracted, making sure that the pieces were composed of sapwood.

The reagents used were ETI SODA (Ciner Group, Istanbul, Turkey), solid-state sodium bicarbonate ($NaHCO_3$), and solid-state calcium chloride ($CaCl_2$) from CASO FCC FLAKES Solvay (Missouri, Il, USA). Absolute ethyl alcohol 99% m/m of the brand Reactivos Químicos Gamma (San José, Costa Rica), distributed by Laboratorios Químicos ARVI S.A, was used.

Mineralization process

The *in-situ* mineralization process was performed in 20 samples (46 cm long × 7.5 cm wide × 2 cm thick), using the vacuum and pressure equipment shown in the diagram in Fig. 1a. The samples were placed into a tank (25 cm diameter × 48 cm length × 27 L capacity) for impregnation with salts. Calcium carbonate ($CaCO_3$) formation (Eq. 1) was performed by means of two impregnation cycles. Figure 1b shows impregnation with $CaCl_2$ (Eq. 2) and impregnation with $NaHCO_3$ (Eq. 3). In the $CaCl_2$ cycle, the wood was impregnated with $CaCl_2$ in an ethanol solution at 1 mol-L^{-1} concentration (Eq. 2), by first applying vacuum at -70 kPa (gauge) for 20 min and then immersing the samples totally into the solution and applying 690 kPa pressure for 30 min (Fig. 1a). In the $NaHCO_3$ cycle, the samples were impregnated with an aqueous solution at 1 mol-L^{-1} concentration (Eq. 2),

by applying vacuum for 20 min, followed by 690 kPa pressure for 50 min. After finishing the first cycle, the samples were washed in distilled water and then were left to dry inside a chamber under controlled conditions (22 °C and 66% relative humidity) until reaching 12% moisture content. After the second cycle, the samples were washed in ethanol and then dried at 40 °C for 4 h. The details of this process can be consulted in Gaitán-Alvarez *et al*. (2020). Equations 1 through 3 are as follows:

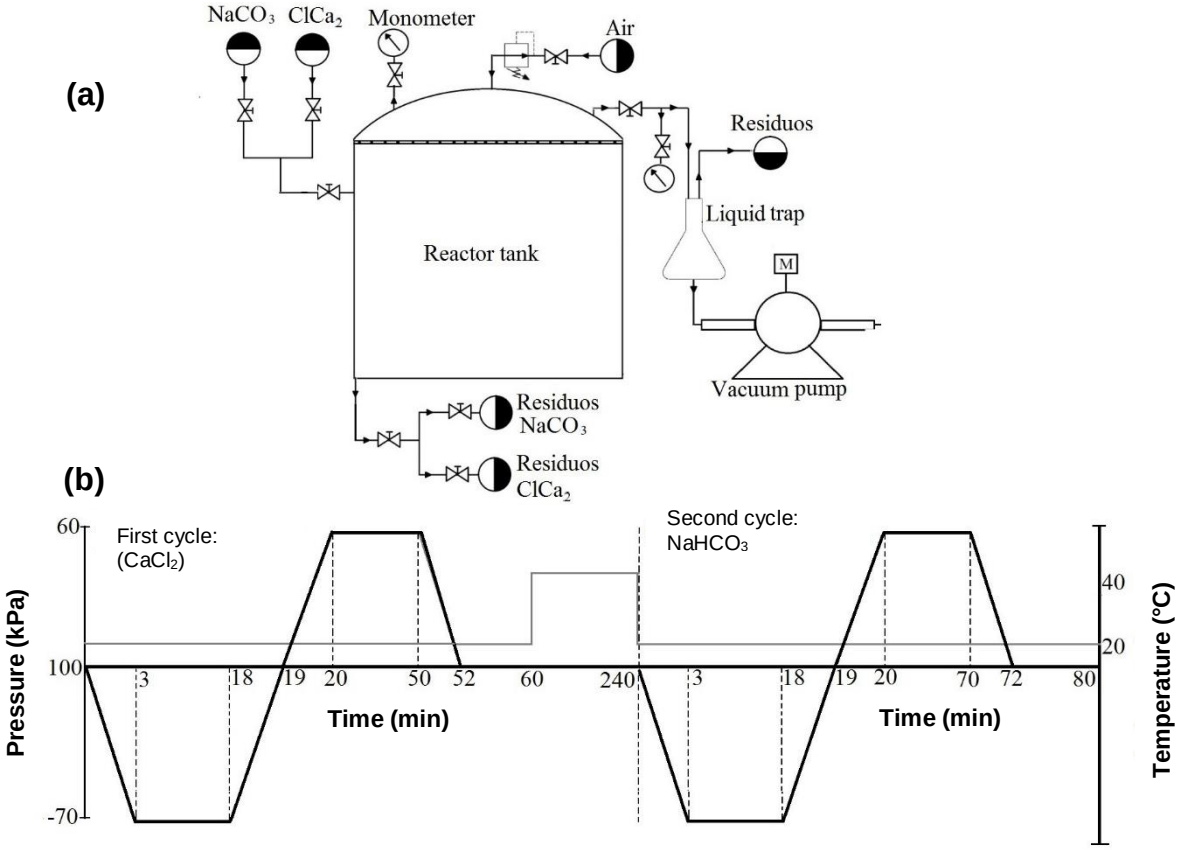

Fig. 1. Flow chart of equipment pressure (a) and flow chart, temperature, and time for *in-situ* mineralization (b) used for *in-situ* mineralization

$$Ca^{2+} + CO_3^{2-} \rightarrow CaCO_3 \quad (1)$$

$$CaCl_2 \times 2H_2O \rightarrow Ca^{2+} + 2Cl^- \quad \text{(ethanol solution)} \quad (2)$$

$$NaHCO_3 \rightarrow Na^+ + H^+ + CO_3^{2-} \quad \text{(aqueous solution)} \quad (3)$$

Methods

Evaluation of the mineralization process

In the $CaCl_2$ cycle, the samples were weighed before and after impregnation with $CaCl_2$. Thus, absorption of the $CaCl_2$ solution (Eq. 4) and salt retention (Eq. 5) were obtained. In the $NaHCO_3$ cycle, again the sample was weighed before and after impregnation with $NaHCO_3$ and again absorption of the $NaHCO_3$ solution (Eq. 4) and salt retention (Eq. 5) were obtained. The details regarding salt retention and $CaCO_3$ formation

can be found in Gaitán-Alvarez *et al.* (2020). Salt absorption and retention were calculated according to Eqs. 4 and 5:

$$\text{Salt absorption } \left(\frac{\text{liters}}{\text{m}^3}\right) = \frac{(Weight_{before\ impreg\ (g)} - Weight_{after\ impreg\ (g)}}{Volume\ of\ sample\ (cm^3)} \times \frac{(100\ \text{cm})^3}{1\ \text{m}^3} \times \frac{1\ \text{L}}{1000\ \text{g}} \quad (4)$$

$$\text{Salt retention } \left(\frac{\text{kg}}{\text{m}^3}\right) = Salt\ absorption\ \left(\frac{L}{m^3}\right) \times \frac{salt\ concentration\ \left(\frac{salt\ weight\ in\ kg}{solution\ weight\ in\ kg}\right)}{solution\ density\ \left(\frac{weight\ in\ kg}{\text{liters}}\right)} \quad (5)$$

Thermogravimetric analysis

The thermogravimetric analysis (TGA) was realized for $CaCO_3$/wood composites and 5 mg previously dried sawdust from untreated/wood was used. The heating rate used was 20 °C min^{-1} from 50 °C to 800 °C, in an ultra-high purity nitrogen atmosphere at a flow of 100 mL min^{-1}. A thermogravimetric analyzer from TA Instruments (Lukens drive, New Castle, USA), model SDT Q600, was used. The TGA gave values of weight loss relative to temperature, these values were used to perform the derivative thermogravimetric analysis (DTG), which was used to obtain the temperature at which the sample was degraded. The TGA data and its derivatives were analyzed using TA Instruments (TA Instruments, Lukens Drive New Castle, USA) Universal Analysis 2000 software.

Physical properties

The following physical properties were determined: density, moisture content (MC), water absorption of immersed wood in water, tangential and radial swelling of wood, and moisture absorption due to changes in the condition of equilibrium moisture content (EMC) (from 12% to 18%). Sample density was determined for 20 $CaCO_3$/wood composites samples and 20 untreated/wood samples; the samples' volume and weight were measured, and then the density (weight/volume) was determined. The MC was calculated for 20 $CaCO_3$/wood composites samples and 20 untreated/wood samples, following the procedures in ASTM D4442-42 (2016). To determine the tangential and radial swelling and the percentage of water absorption, 20 samples 5 × 5 × 2 cm from each treatment were conditioned and weighed at 12% EMC and then conditioned for a period of 3 to 4 weeks at 18% EMC. After conditioning, the samples were weighed and measured again. This procedure was based on the ASTM D4933-99 (1999) standard but modified to the conditions in Costa Rica, where environmental moisture conditions are approximately 18%. Tangential and radial swelling were calculated using Eq. 6. Moisture absorption was determined through Eq. 8 by obtaining first 12% and 18% moisture content with respect to dry weight (Eq. 7). The difference between both moisture measurements (12% and 18%) represented sample moisture absorption (Eq. 8):

$$\text{Swelling (mm)} = \text{(g)}\ \frac{measurement 12\%\ (mm) - measurement 18\%\ (mm)}{measurement\ 12\%\ (mm)} \times 100 \quad (6)$$

$$\text{Moisture content}_{\text{MC}} = \frac{Weight_{MC}\ (g) - Weight_{oven\ dried}\ (g)}{Weight_{oven\ dried}\ (g)} \times 100 \quad (7)$$

$$\text{Moisture absorption} = Moisture\ content_{18\%} - Moisture\ content_{12\%} \quad (8)$$

For weight gain from water immersion, 20 samples for each species/treatment previously weighed were immersed in water for 24 h. After this period, the samples were

weighed and the weight gain was determined following Eq. 7, according to ASTM D4446-13 (1985).

Mechanical properties

The mechanical properties analyzed were resistance to static flexure and grain parallel compression. In both tests, procedure B described in ASTM D143 (2016) was used. Twenty samples were taken from each species/treatment for each one of the tests. The tests were performed in a testing machine Tinius Olsen model H10KT (Tinius Olsen Test Machine Company, Horsham, PA, USA) in the case of static flexure and Tinius Olsen L60 (Tinius Olsen Test Machine Company, Horsham PA, USA) for compression.

Fire retardancy

For this test, 10 $CaCO_3$/wood composite samples and 10 untreated/wood samples were used for each species. The sample size was 15 cm in length × 10 cm in width × 9 mm in thickness, in accordance with the methodology proposed by Taghiyari (2012). The samples were placed in the device specially designed for this test. Once the sample was placed at an angle of 45° and 27 mm from the flame, the test timing began, as follows: (i) dark time, the moment when the back of the sample exposed to the flame began to form a dark spot; (ii) hole time, the time when a hole begins to appear on the back of the sample exposed to fire; (iii) flame time, the moment when the flame begins to appear on the surface exposed to fire; (iv) ember time, when the embers begin to appear around the burning hole; and (v) end time, the time when the test stops, when most of the surface of the sample has already been consumed by fire. Weight loss was also recorded during the curfew test, recording the weight before and after the test.

Durability

The methodology in ASTM D2017-81 (1995) was used to perform the test of resistance to natural decay. In each treatment/species, 40 samples, 2 cm wide × 2 cm long × 2 cm thick were prepared. Two types of fungi were used for this test, *Trametes versicolor* and *Lenzites acuta*, corresponding to white and brown rot, respectively. Both fungi are of university collection, usually used in assessment of decay resistance wood (TEC, Cartago, Costa Rica). Twenty samples per species/treatment were subjected to degradation by each one of the fungi, for a period of 12 weeks.

Statistical Analysis

The statistical analysis consisted primarily of checking the normality and homogeneity of the data and the elimination of outliers. Then, the descriptive analysis consisted of determining the mean, standard deviation, and coefficient of variation for each variable studied for each species and treatment. For each variable evaluated, an analysis of variance (ANOVA) was performed with a level of statistical significance of $p < 0.05$ to determine variability in response to the mineralization treatment. Tukey's test was used to determine the statistical significance of the differences between the means of the variables. This analysis was done with the SAS 9.4 program (SAS Institute Inc., Cary, NC, USA).

RESULTS AND DISCUSSION

Absorbed amounts of the solutions of $CaCl_2$ and $NaCO_3$ in the different species ranged from 42.2 to 168.0 L/m^3 and 69.5 to 214.6 L/m^3 (Table 1), respectively. The ANOVA for these two parameters showed that absorption of the $CaCl_2$ solution *in-situ* was higher in *Ec*, *Ha*, *Ss*, *Vf*, and *Vg*, while lower absorptions were observed in *Co*, *Ga*, and *Tg* (Table 1). Meanwhile, absorption of the $NaCO_3$ solution appeared in greater quantities in *Ha*, *Ss*, and *Vf*; and in lesser quantities in *Co*, *Ga*, and *Tg* (Table 1). Additionally, $CaCO_3$ retention *in-situ* ranged from 2.8 to 9.2 kg/m^3 and was greater in *Ec*, *Ha*, *Ss*, *Vf*, and *Vg*, and smaller in *Co*, *Ga*, and *Tg*, with statistical differences between them (Table 1). Details of the formation and location of $CaCO_3$ crystals can be found in Gaitán-Alvarez *et al.* (2020), and Fig. 2 shows the salt formation in *E. cyclocarpum*, with greater formation and *C. odorata* with lower salt formation (Table 1). As for unreacted salts in the wood, surplus ions of Ca^{2+} and CO_3^{2+} could be observed within the same species, reaching up to 40% of the treated species (Table 1). A surplus of Ca^{2+} ions was observed in *Ca*, *Ec*, *Ss*, and *Vg*, while in *Ca*, *Ga*, *Ha*, *Tg*, and *Vf* the surplus ions were CO_3^{2+}. As for the amount of unreacted salt relative to volume, *Ec* presented the highest values with 3.8 and 6.0 g/m^3 of CO_3^{2-} and Ca^{2+}, respectively, followed by *Vf* and *Vg*. The wood with less amounts of unreacted salts were *Co* and *Ca* wood (Table 1).

Table 1. Absorption of $CaCl_2$ and $NaCO_3$, and Retention of $CaCO_3$ Estimated in the *in-situ* Mineralization Process of Nine Woods from Fast-growth Tropical Species in Costa Rica

Wood	$CaCl_2$ Absorption (L/m^3)	$NaCO_3$ Absorption (L/m^3)	$CaCO_3$ Amount *in situ* (kg/m^3)	Unreacted Ca^{2+} (g/m^3)	Unreacted CO_3^{2-} (g/m^3)
Cedrela odorata	51.0 (13.4)^{A}	87.8 (14.1)^{A}	2.8 (0.7)^{A}	0.21 (131.76)	0.93 (43.11)
Cordia alliodora	123.9 (42.1)^{B}	152.7 (43.4)^{B}	6.6 (2.3)^{B}	1.21 (106.66)	0.73 (85.19)
Enterolobium cyclocarpum	167.9 (106.7)^{C}	175.4 (73.9)^{BC}	9.2 (5.8)^{C}	3.83 (146.14)	6.05 (128.94)
Gmelina arborea	50.3 (3 .7)^{A}	69.5 (53.3)^{A}	2.4 (1.8)^{A}	1.72 (95.97)	1.60 (66.10)
Hyeronima alchorneoides	150.2 (56.9)^{BC}	195.1 (56.8)^{CDE}	8.2 (3.1)^{BC}	1.65 (75.15)	1.12 (85.08)
Samanea samans	157.3 (25.4)^{BC}	208.1 (51.4)^{D}	8.6 (1.4)^{BC}	1.44 (74.21)	1.84 (40.16)
Tectona grandis	42.2 (32.3)^{A}	72.3 (14.3)^{A}	2.6 (1.8)^{A}	2.47 (97.00)	1.05 (45.54)
Vochysia ferruginea	158.1 (85.7)^{BC}	214.6 (67.8)^{D}	8.6 (4.7)^{BC}	3.15 (80.17)	3.66 (77.09)
Vochysia guatemalensis	136.7 (30.7)^{BC}	177.2 (67.0)^{EB}	7.5 (1.7)^{BC}	1.61 (63.14)	2.21 (123.87)

The numbers in parentheses represent variation coefficients, and different letters in each parameter represent significant statistical differences ($p < 0.05$).

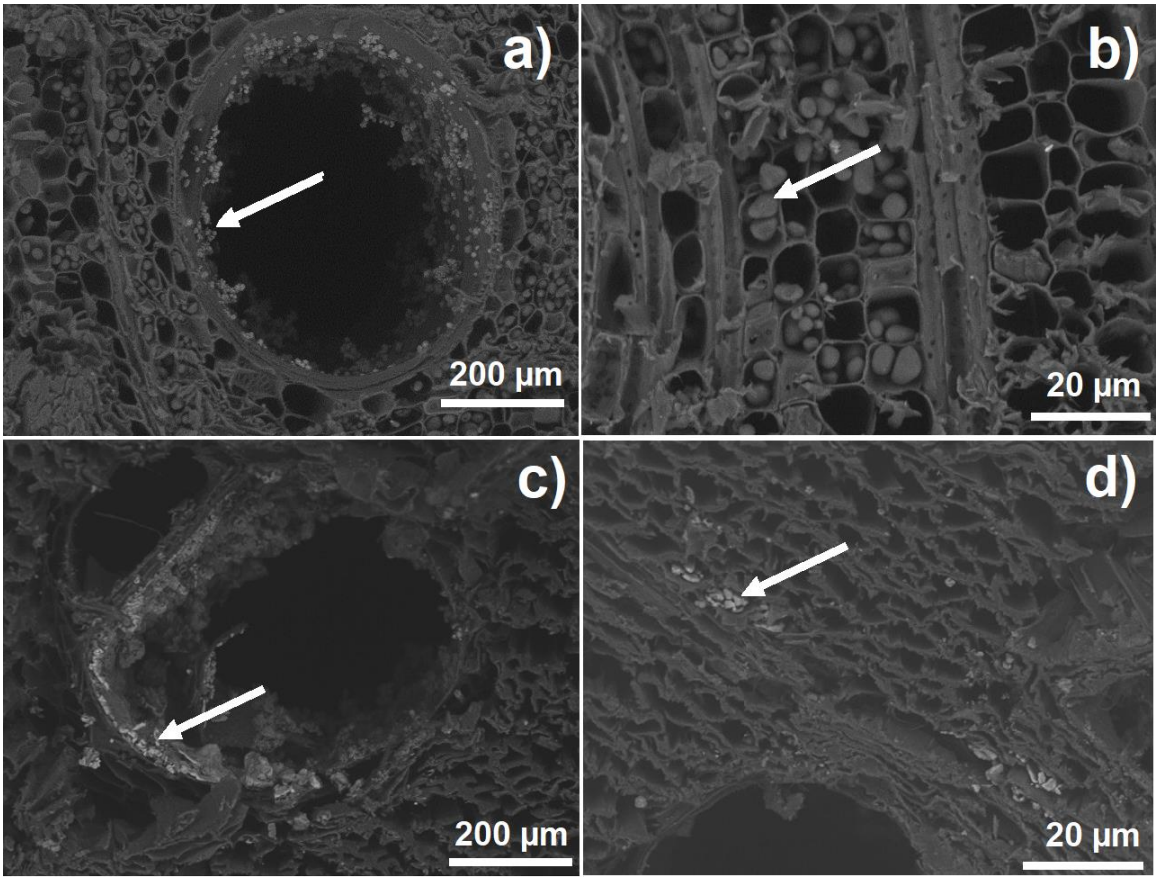

Fig. 2. SEM images showing in-situ $CaCO_3$ formation in different anatomical features in *E. cyclocarpum* with highest salt formation and *C. odorata* with lowest salt formation: High quantity of $CaCO_3$ crystals formed in lumina of vessels (a) and in lumina ray parenchyma (b) of *E. cyclocarpum* and lower of $CaCO_3$ crystals formed in lumina of vessels (a) and in lumina ray parenchyma (b) of *C. odorata*. Arrow shows $CaCO_3$ crystals.

Although adequate absorptions were achieved to have the number of ions (Ca^{2+} or CO_3^{2+}) sufficient for $CaCO_3$ formation, the stoichiometry is not suitable for the formation of this salt (Table 1). Salt formation is a complex mechanism that includes the polymorphism exhibited by crystals of calcium carbonate, calcium oxalate, and different polymorphs of the same compound that can transform into each other. Crystal formation also influences the environmental temperature, concentration, pH, viscosity, additives, and so on (Zeng *et al*. 2018), which are conditions difficult to control in processes and equipment used in commercial preservation intended for application in wood mineralization.

Thermogravimetric Analysis

The TGA of the two different salts used for *in-situ* $CaCO_3$ formation showed that for $CaCl_2$ used in the first cycle, decomposition occurred in two phases: the first phase with the highest peak at 149 °C and the second phase with the highest peak at 200 °C (Fig. 3a).

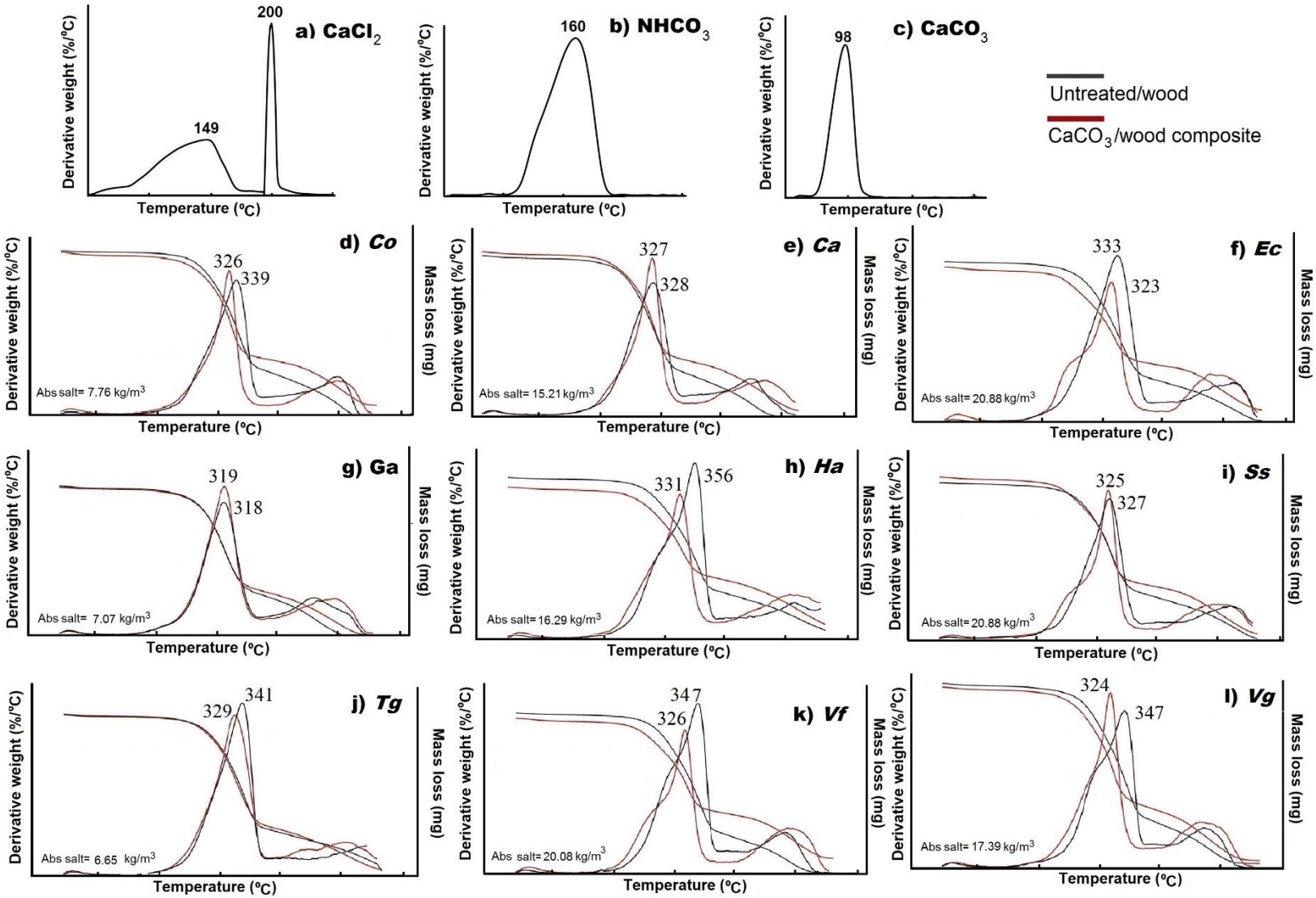

Fig. 3. TGA and DTG analysis of $CaCO_3$/wood composites and untreated/wood of nine fast growth tropical species in Costa Rica

Regarding $NaHCO_3$, decomposition occurred in one phase, with the highest peak showing at 160 °C (Fig. 3b). In $CaCO_3$, decomposition occurred in only one phase, with the maximum peak at 98 °C (Fig. 3c).

In relation to $CaCO_3$/wood composites, thermal decomposition of the nine woods showed the same pattern of untreated wood in the TGA; however, the DTG curve showed differences in the $CaCO_3$/wood composites of the various species (Fig. 3a through l). The DTG curve presented three important decomposition stages: the first one appeared as a signal in the form of a slight curve after 200 °C; the second stage showed at the highest peak of decompositions between 320 °C and 360 °C; and the third as a slight signal at the end after 380 °C (Fig. 3d through l). All of the woods studied showed that the maximum decomposition peak of the $CaCO_3$/wood composites occurred before untreated/wood (Fig. 3d through l). The DTG curve also showed that in the woods with higher $CaCO_3$ formation (*Ec*, *Ss*, *Vf*, and *Vg*) the signal at 200 °C was more pronounced than the signal of untreated/wood at 200 °C (Fig. 3f, i, k, and l). Meanwhile, in the species with average retention (15.2 to 17.4 kg/m^3), such as *Ca* and *Ha* wood, the pronunciation of the curve at 200 °C was slight, almost similar to untreated/wood (Fig. 3c and h). Additionally, $CaCO_3$/wood composites of *Co*, *Ga*, and *Tg* wood that presented the smallest values of $CaCO_3$ retention, followed the same behavior of untreated/wood (Fig. 3e, g, and j).

The TGA results showed that, except for *Co* and *Ss*, at the beginning $CaCO_3$/wood composites of the species lost weight faster than untreated/wood; however, after 350 °C the opposite behaviour occurred: untreated/wood lost weight faster (Fig. 3d through 3l). This effect was more pronounced in $CaCO_3$/wood composites above 16.29 kg/m^3 (*Ec*, *Ha*, *Ss*, *Vf*, and *Vg*) (Fig. 3f, 3h, 3i, 3k, and 3l). These results agree with those obtained by Tsioptsias and Pnayiotou (2011), who found the same behavior in $CaCO_3$/wood composites of *Picea abies*. Fast initial degradation of $CaCO_3$/wood composites was due to early endothermal degradation of $CaCO_3$, water, and CO_2 (Dash *et al.* 2000), where most degradation occurred before reaching 100 °C (Fig. 3c). However, at higher temperatures (> 350 °C), $CaCO_3$/wood composites turned more stable to combustion due to aragonite transforming into calcite at 387 °C (Brown and Gallagher 2003), which decomposed into CaO and CO_2 at temperatures above 850 °C (Singh and Singh 2007).

Fire Resistance

In relation to flame time, $CaCO_3$/wood composites of *Ca*, *Ec*, *Ha*, and *Vg* needed more time than untreated/wood of the same species (Table 2). The remaining species (*Ca*, *Ga*, *Sa*, *Tg*, and *Vf*) showed no statistical differences between $CaCO_3$/wood composites and untreated/wood (Table 2). Ember time varied again between species and was statistically higher in $CaCO_3$/wood composites of *Co*, *Ec*, *Ha*, and *Ss* in relation to untreated/wood. In $CaCO_3$/wood composites of *Ha* and *Tg*, ember time was shorter than in untreated/wood. No statistical differences appeared in the remaining species (*Ca*, *Ga*, *Vf*, and *Vg*) (Table 2). Dark time and hole time were not statistically affected between $CaCO_3$/wood composites and untreated/wood of *Ca*, *Ec*, *Ga*, *Ha*, *Vf*, and *Vg*. Dark time increased statistically in $CaCO_3$/wood composites of *Ca* and *Ss* but diminished statistically in $CaCO_3$/wood composites of *Tg* (Table 2). Lastly, the total testing time varied with the type of wood (Fig. 4b). *Ca*, *Ga*, *Vf*, and *Vg* woods showed no statistical differences between $CaCO_3$/wood composites and untreated/wood (Fig. 4b). The end time in $CaCO_3$/wood composites of *Co*, *Ec*, and *Ss* was statistically higher than in untreated/wood. In contrast, in $CaCO_3$/wood composites of *Ha* and *Tg*, the end time was statistically lower than in untreated/wood (Fig. 4b).

Table 2. Different Times in the Fire-retardancy Test of $CaCO_3$/Wood Composites and Untreated/Wood of Nine Fast-growth Tropical Species in Costa Rica

Species	Treatment	Flame Time (min)	Ember Time (min)	Dark Time (min)	Hole Time (min)
Co	$CaCO_3$/wood composite	0.8 (48.1)^A	2.3 (37.6)^A	23.0 (27.6)^A	29.9 (59.7)^A
	Untreated/wood	0.4 (11.6)^A	1.1 (11.5)^B	12.7 (21.0)^B	24.1 (9.6)^B
Ca	$CaCO_3$/wood composite	0.9 (26.4)^A	2.0 (31.9)^A	23.8 (10.9)^A	36.0 (8.8)^A
	Untreated/wood	0.5 (57.1)^B	1.5 (23.9)^A	23.5 (21.1)^A	33.2 (29.2)^A
Ec	$CaCO_3$/wood composite	1.4 (31.4)^A	5.5 (56.3)^A	26.7 (19.1)^A	37.4 (10.8)^A
	Untreated/wood	0.6 (47.6)^B	2.8 (34.1)^B	23.1 (8.3)^A	32.3 (7.8)^B
Ga	$CaCO_3$/wood composite	0.6 (62.2)^A	1.9 (22.4)^A	24.7 (24.1)^A	37.6 (16.9)^A
	Untreated/wood	0.8 (44.2)^A	2.6 (25.7)^A	21.7 (30.4)^A	36.4 (28.4)^A
Ha	$CaCO_3$/wood composite	1.9 (23.3)^A	3.2 (4.7)^A	20.2 (11.7)^A	53.9 (6.7)^A
	Untreated/wood	1.2 (11.0)^B	5.4 (17.7)^B	18.8 (11.1)^A	83.4 (19.5)^B
Ss	$CaCO_3$/wood composite	2.8 (14.0)^A	7.8 (27.0)^A	45.3 (11.5)^A	60.2 (5.5)^A
	Untreated/wood	2.2 (20.6)^A	4.7 (32.3)^B	12.2 (6.6)^B	28.4 (22.3)^B
Tg	$CaCO_3$/wood composite	1.1 (18.4)^A	2.8 (18.4)^A	25.2 (13.9)^A	40.1 (13.5)^A
	Untreated/wood	1.3 (7.4)^A	6.2 (6.0)^B	57.2 (19.6)^B	79.7 (28.5)^B
Vf	$CaCO_3$/wood composite	0.7 (47.0)^A	2.6 (35.5)^A	34.8 (12.7)^A	49.3 (23.8)^A
	Untreated/wood	0.7 (43.1)^A	1.8 (31.7)^A	34.3 (5.2)^A	63.5 (29.6)^A
Vg	$CaCO_3$/wood composite	0.9 (24.4)^A	1.9 (18.6)^A	35.2 (13.2)^A	86.1 (37.5)^A
	Untreated/wood	0.4 (36.7)^B	1.7 (27.0)^A	30.9 (2.7)^A	58.1 (33.3)^A

The numbers in parentheses represent variation coefficients and different letters in each parameter represent significant statistical differences ($p < 0.05$)

The evaluation of the weight loss at the end of the flame test demonstrated that all the mineralized woods showed less weight loss relative to untreated/wood; however, in $CaCO_3$/wood composites of *Ss* wood the weight loss was statistically higher than in $CaCO_3$/wood composites (Fig. 4b).

The fire resistance analysis confirmed the previous results. $CaCO_3$/wood composites of species showing greater *in-situ* $CaCO_3$ formation, such as *Ec*, *Ss*, *Vf*, and *Vg* (Table 1), resisted fire better (Fig. 4; Table 2). These results agree with those obtained by Merk *et al.* (2015, 2016) and Tsioptsias and Panayiotou (2011) in $CaCO_3$/wood composites of beech and spruce. Merk *et al.* (2015) explained that impregnating the wood with $CaCO_3$ affects the thermal decomposition of the cellulose by reducing the formation of volatiles. Similarly, Yao *et al.* (2008) indicated that minerals embedded in the tissues dilute the

amount of fuel material and constitute a barrier to heat transmission and weight transport during pyrolysis. However, other authors (Walters and Lyon 2003; Hull *et al.* 2011) indicated that $CaCO_3$ limits the supply of oxygen and volatile material. Therefore, incrementing the quantity of embedded $CaCO_3$ crystals in *Ec*, *Ss*, *Vf*, and *Vg* reduces the flammability of the mineralized material and increases its thermal stability and fire resistance (Fig. 3; Table 2).

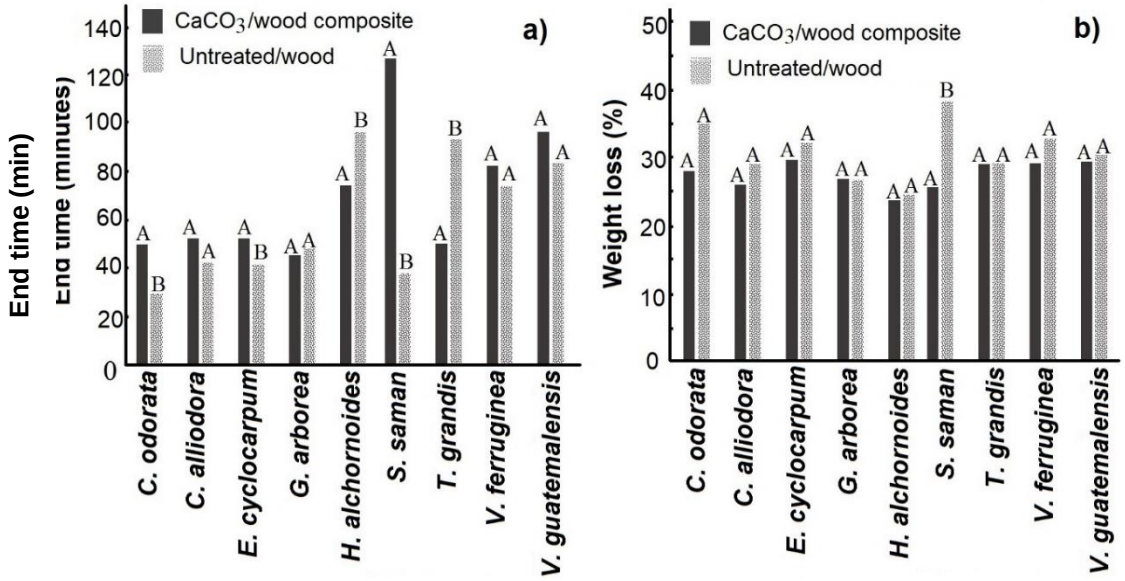

Fig. 4. End time (a) and weight loss (b) in the fire retardancy test of $CaCO_3$/wood composites and untreated/wood of nine fast growth tropical species in Costa Rica; different letters in each parameter represent significant statistical differences ($p < 0.05$)

Physical Properties

Table 3 shows the values of the physical properties of $CaCO_3$/wood composites and untreated/wood. In regard to density, $CaCO_3$/wood composite of *Ca* was the only one to present a statistical difference higher than in untreated/wood. The MC in $CaCO_3$/wood composites of *Ec*, *Ss*, *Vf*, and *Vg* was statistically higher than untreated/wood, while the remaining woods showed no statistical differences. Moisture absorption was from 12% to 18% in all woods. The percentage of absorption was statistically higher in $CaCO_3$/wood composites than in untreated/wood (Table 3). As for water absorption by immersion, in all the species studied except *Vg*, $CaCO_3$/wood composite presented a statistically higher percentage of absorbed water than in untreated wood (Fig. 5). In relation with different swelling, it was found that the width swelling was statistically lower only in untreated/wood of *Ha* than in untreated/wood. Meanwhile, $CaCO_3$/wood composites of *Ec* and *Ga* presented higher thickness swelling than untreated/wood (Table 3).

Regarding the physical properties, the results showed that the mineralization process did not affect the density and the MC of wood (Table 2). Lack of differences between $CaCO_3$/wood composites and untreated/wood was explained by the fact that the quantity of *in situ* formed $CaCO_3$ (Table 1), between 2.8 and 9.2 kg/m^3, was slightly significant for the values of wood density before the process of mineralization, which varied between 266 and 550 kg/m^3. Likewise, similarities between treated and untreated wood suggested that the structural components (or other types) of the wood (cellulose,

hemicellulose, and lignin) were not significantly affected by the chemical substances (water and ethanol) used in the *in-situ* mineralization process.

Table 3. Some Physical Properties Evaluated of $CaCO_3$/Wood Composites and Untreated/Wood of Nine Fast-growth Tropical Species in Costa Rica

Species	Treatment	Density (g/cm^3)	Moisture Content (%)	Moisture Absorption (%)	Width Swelling (mm)	Thickness Swelling (mm)
Co	$CaCO_3$/wood composite	257.3 (8.0)^A	12.8 (40.5)^A	4.2 (10.7)^A	0.5 (17.3)^A	0.6 (63.4)^A
	Untreated/wood	266.4 (8.1)^A	10.9 (58.3)^A	1.5 (9.9)^B	0.4 (114.3)^A	0.3 (1.8)^A
Ca	$CaCO_3$/wood composite	387.26 (6.7)^A	11.8 (13.4)^A	4.6 (24.0)^A	0.8 (33.1)^A	0.7 (118.4)^A
	Untreated/wood	341.2 (11.4)^B	10.9 (7.5)^A	2.7 (8.3)^B	0.8 (73.1)^A	1.2 (83.3)^A
Ec	$CaCO_3$/wood composite	397.9 (15.9)^A	12.6 (13.8)^A	8.2 (30.4)^A	1.6 (74.8)^A	0.4 (126.6)^A
	Untreated/wood	395.5 (10.3)^A	11.2 (11.4)^B	4.2 (19.4)^B	1.6 (57.9)^A	0.9 (93.4)^B
Ga	$CaCO_3$/wood composite	400.9 (10.1)^A	12.0 (14.9)^A	2.6 (44.6)^A	0.5 (66.0)^A	0.3 (100.6)^A
	Untreated/wood	418.9 (9.3)^A	13.5 (7.6)^A	1.6 (41.8)^B	0.3 (142.3)^A	0.6 (57.9)^B
Ha	$CaCO_3$/wood composite	541.8 (9.5)^A	11.4 (34.9)^A	3.5 (12.9)^A	0.4 (104.8)^A	0.8 (72.8)^A
	Untreated/wood	518.9 (5.1)^A	12.7 (4.3)^A	2.2 (15.0)^B	0.7 (51.6)^B	1.3 (83.4)^A
Ss	$CaCO_3$/wood composite	535.2 (4.7)^A	11.5 (8.1)^A	6.7 (30.4)^A	1.6 (71.8)^A	0.6 (75.8)^A
	Untreated/wood	521.6 (5.1)^A	10.8 (4.1)^B	3.9 (19.4)^B	2.1 (43.1)^A	0.8 (81.4)^A
Tg	$CaCO_3$/wood composite	544.8 (10.5)^A	11.9 (16.6)^A	5.2 (23.4)^A	2.5 (117.8)^A	0.9 (90.3)^A
	Untreated/wood	541.9 (9.7)^A	11.8 (11.6)^A	4.4 (6.2)^B	2.2 (45.4)^A	1.5 (73.9)^A
Vf	$CaCO_3$/wood composite	321.9 (7.0)^A	11.9 (7.0)^A	6.6 (32.5)^A	1.1 (66.6)^A	0.5 (112.7)^A
	Untreated/wood	317.8 (9.7)^A	9.2 (35.9)^B	3.0 (9.6)^B	0.8 (77.4)^A	0.8 (49.7)^A
Vg	$CaCO_3$/wood composite	297.7 (7.4)^A	11.2 (10.7)^A	8.5 (11.9)^A	3.9 (112.9)^A	0.9 (93.9)^A
	Untreated/wood	304.9 (6.0)^A	9.7 (8.0)^B	4.8 (7.7)^B	3.4 (40.2)^A	1.2 (77.5)^A

The numbers in parentheses represent variation coefficients and different letters in each parameter represent significant statistical differences ($p < 0.05$)

In those species where MC values were statistically affected, it showed a reduction. This was because the $CaCO_3$ crystals adhered to the cell wall, creating bonds with the hydroxyl groups of the wall (Butylina *et al*. 2012; Merk *et al*. 2016), and preventing association of these groups with water molecules present in the environment or making water molecules associate with more hydroxyl groups in the outer side of the wood, so that cell wall swelling would diminish (Stark and Gardner 2008). The obstacle posed by the affinity of the $CaCO_3$/wood composites produced a reduction of the wood's equilibrium

moisture content when exposed to temperature and relative humidity close to 12%, which the samples were conditioned to, after *in-situ* $CaCO_3$ formation.

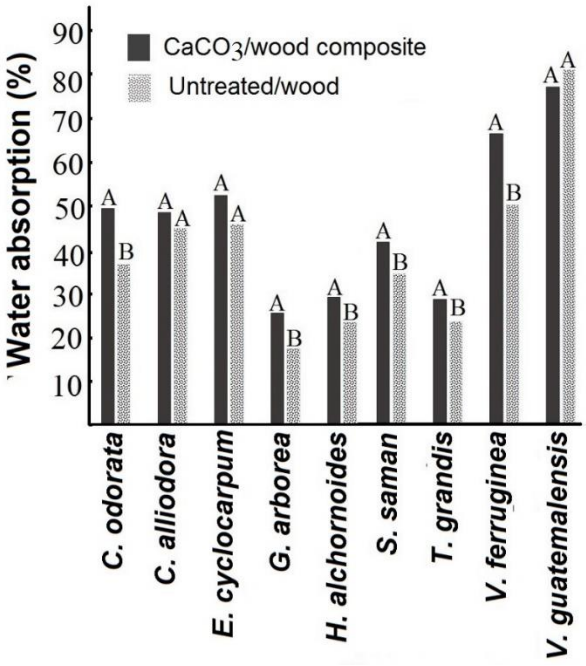

Fig. 5. Water absorption by immersion of $CaCO_3$/wood composites and untreated/wood of nine fast-growth tropical species in Costa Rica; different letters in each parameter represent significant statistical differences ($p < 0.05$).

A remarkable aspect of the results of physical properties of $CaCO_3$/wood composites of tropical woods in fast growing plantations was the increase in moisture absorption, from 12% to 18%, and water absorption after immersing 24 h in water (Table 2; Fig. 5), which contradicts the studies conducted by Merk *et al.* (2015, 2016). This contradiction may be explained by lack the of efficiency of the method of *in-situ* $CaCO_3$ formation in wood samples in which permeability plays an important role; or, CaCO3 crystal formation in specific sites (vessel lumina, rays, and axial parenchyma) of the hierarchical structure of the wood (Gaitán-Álvarez *et al.* 2020). As found in this study, in the process of mineralization there was a percentage of NaCl or small quantities of unreacted Ca^{2+} and CO_3^{2-} (Gaitán-Álvarez *et al.* 2020) that probably remained deposited in the wood (Merk *et al.* 2016). These salts are highly water soluble (Harvie *et al.* 1984), enabling $CaCO_3$/wood composites to absorb more water, as occurred with composites of several species (Table 1). In fact, $CaCO_3$/wood composites of the species with higher percentage of unreacted salts (*Ec*, *Ss*, *Vf*, and *Vg*) presented the highest percentage of moisture absorption in the samples impregnated (Fig. 6). These results suggest that salts, instead of the wood structure, retained the absorbed water and that the process of formation *in situ* should be improved for bigger wood samples.

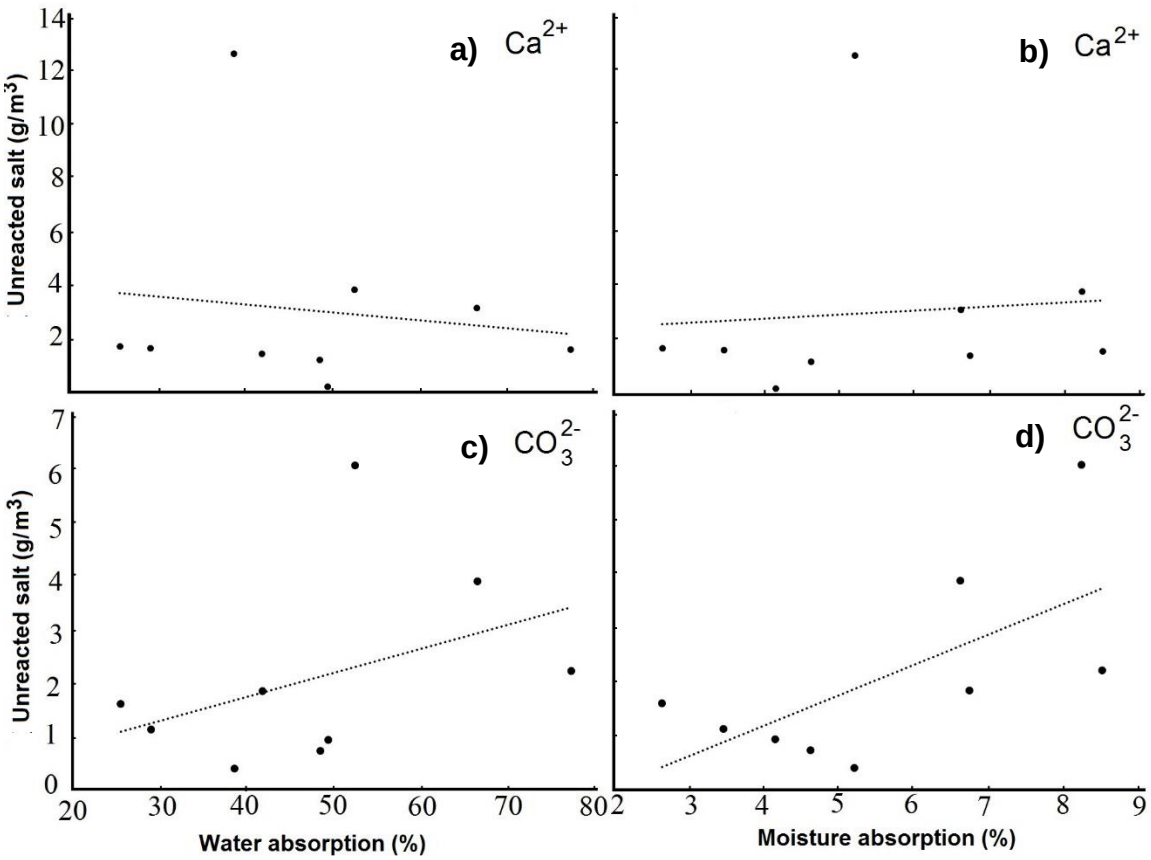

Fig. 6. Correlation between unreacted salts and water absorption (a, c) and moisture absorption (b, d)

The scarce difference in swelling (width and thickness) between treated and untreated wood suggests that high water absorption in $CaCO_3$/wood composites was associated with $CaCl_2$ and $NaCO_3$ salts that did not react to form $CaCO_3$. Although high moisture absorption (Table 2) was observed, few species presented statistical difference in swelling, or remained the same in both the impregnated and untreated samples (Table 2). This situation could be explained by the fact that calcium carbonate crystals adhered to the cell wall creating bonds with the hydroxyl groups of the wall (Butylina *et al.* 2012), hindering association with moisture.

Mechanical Properties

The mechanical properties of $CaCO_3$/wood composites and untreated/wood presented few significant differences, except for mineralized wood of Ca regarding flexural modulus of rupture (MOR) and modulus of elasticity (MOE) and compression MOR, which were statistically higher than in untreated/wood (Table 4); and $CaCO_3$/wood composites of *Ss*, in which flexural MOR and MOE diminished statistically (Table 4).

It has been affirmed that adding mineral to the structure of cellulose, such as $CaCO_3$, improves the mechanical properties of flexion, compression, and tension of materials (Hadal *et al.* 2004; Huuhilo *et al.* 2010) or wood-plastic composites (Leong *et al.* 2004; Sun *et al.* 2006; Cheng *et al.* 2015). However, this study disagrees with that affirmation because the results showed that there were few changes in the mechanical properties (Table 3). This lack of agreement of the results of this study with those of other

studies shows that the effects of $CaCO_3$ formation on mechanical properties of solid wood are scarcely known and that formation of this mineral in wood composites will have little effect on the wood properties (Table 3).

Table 4. Mechanical Properties of $CaCO_3$/Wood Composites and Untreated/ Wood of Nine Fast-growth Tropical Species in Costa Rica

Species	Treatment	Flexion Test		Compression Test	
		MOR (MPa)	MOE (GPa)	MOR (MPa)	MOE (GPa)
Co	$CaCO_3$/wood composite	35.9 (9.9)^A	5.4 (15.6)^A	29.9 (25.3)^A	0.9 (20.0)^A
	Untreated/wood	34.9 (11.1)^A	5.6 (13.9)^A	31.9 (16.5)^A	0.9 (27.1)^A
Ca	$CaCO_3$/wood composite	58.2 (10.8)^A	8.4 (9.5)^A	40.0 (11.1)^A	0.9 (24.2)^A
	Untreated/wood	47.3 (20.9)^B	6.6 (24.9)^B	29.7 (28.4)^B	0.7 (51.4)^A
Ec	$CaCO_3$/wood composite	37.1 (38.7)^A	4.1 (30.3)^A	14.3 (44.3)^A	21.9 (91.7)^A
	Untreated/wood	38.3 (23.9)^A	4.6 (26.6)^A	16.2 (26.4)^A	13.6 (72.4)^A
Ga	$CaCO_3$/wood composite	58.8 (16.1)^A	8.3 (22.9)^A	43.6 (13.3)^A	1.9 (20.7)^A
	Untreated/wood	58.3 (18.4)^A	9.0 (18.6)^A	36.5 (29.2)^B	1.6 (30.4)^A
Ha	$CaCO_3$/wood composite	72.4 (17.0)^A	9.6 (23.9)^A	38.1 (16.7)^A	1.8 (57.4)^A
	Untreated/wood	75.6 (14.0)^A	10.3 (18.6)^A	35.4 (16.6)^A	1.4 (29.4)^A
Ss	$CaCO_3$/wood composite	60.9 (15.4)^A	6.4 (12.0)^A	23.8 (31.3)^A	21.9 (91.7)^A
	Untreated/wood	68.4 (10.9)^B	7.3 (11.5)^B	27.6 (21.3)^A	13.6 (72.4)^A
Tg	$CaCO_3$/wood composite	82.2 (8.8)^A	10.2 (15.0)^A	29.2 (31.5)^A	36.8 (69.0)^A
	Untreated/wood	79.5 (14.3)^A	9.5 (21.0)^A	29.4 (20.5)^A	30.0 (82.6)^A
Vf	$CaCO_3$/wood composite	34.8 (13.2)^A	5.7 (16.0)^A	31.6 (12.5)^A	0.9 (36.5)^A
	Untreated/wood	35.9 (13.3)^A	5.8 (12.5)^A	29.6 (34.4)^A	0.9 (38.0)^A
Vg	$CaCO_3$/wood composite	31.2 (14.2)^A	4.7 (16.7)^A	14.9 (12.3)^A	6.8 (63.6)^A
	Untreated/wood	34.0 (14.9)^B	4.9 (16.2)^A	16.9 (18.9)^B	7.2 (41.1)^A

The numbers in parentheses represent variation coefficients and different letters in each parameter represent significant statistical differences ($p < 0.05$)

Decay Durability

As for resistance to brown fungus (*L. acuta*) decay, the weight loss percentage was statistically higher in $CaCO_3$/wood composites of *Ca* and *Ec* than in untreated/wood, while $CaCO_3$/wood composites of *Ha* presented less weight loss than untreated/wood (Fig. 7a). As for weight loss due to decomposition caused by *T. versicolor*, no differences appeared between $CaCO_3$/wood composites and untreated/wood of *Co*, *Ga*, *Ha*, *Tg*, *Vf*, and *Vg*, while $CaCO_3$/wood composites of *Ca*, *Ec*, and *Ss*, presented weight loss statistically higher than in untreated/wood (Fig. 7b).

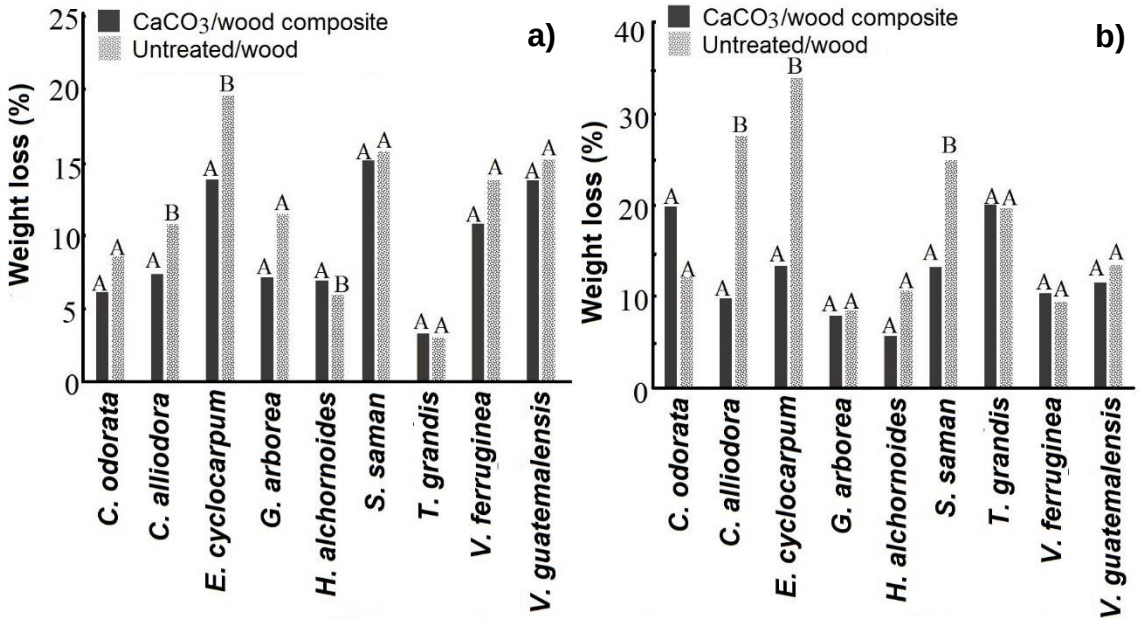

Fig. 7. Weight loss due to natural decay to *Lenzites acuta* (a) and *Trametes versicolor* (b) of $CaCO_3$/wood composites and untreated/wood of nine fast growth tropical species in Costa Rica; different letters in each parameter represent significant statistical differences ($p < 0.05$)

Although the addition of $CaCO_3$ to increase wood durability has been used (Steenkjær Hastrup *et al*. 2006), the effect of this salt ($CaCO_3$) on decay resistance in tropical species was not regular for all wood species tested nor for the type of fungus used. For *L. acuta*, $CaCO_3$/wood composites showed greater weight loss in *Ca* and *Ec* woods than in untreated/wood, while with *T. versicolor* the weight loss was also greater in $CaCO_3$/wood composites of *Ca*, *Ec*, and *Ss* (Fig. 7). Because these results are not acceptably efficient, the performance of the application of mineralization as an alternative to wood decay should be evaluated.

CONCLUSIONS

1. According to the results, the deposit of $CaCO_3$ crystals in the cell structure of hardwoods influences differently the wood properties in the different species tested, probably because of the irregularity of the deposit. *In-situ* $CaCO_3$ mineralization increased water absorption, but it also increased the dimensional stability, with little effect on the mechanical properties and decay resistance of some wood species; however, the major advantage of this treatment was that $CaCO_3$/wood composites exhibited increased fire resistance, as it created a barrier that hindered the exchange of oxygen and volatile material with the outer environment.
2. Mineralization can be completed in tropical hardwood species, but each species will show a different behavior, so the effects on each species must be studied. Despite this, mineralization is a promising treatment to solve the problems of dimensional stability and fire resistance of forest plantation woods.

ACKNOWLEDGMENTS

The authors wish to thank the Vicerrectoría de Investigación y Extensión at the Instituto Tecnológico de Costa Rica (ITCR) for the project financing. The authors thanks María Teresa Vargas L. for translation and editing of English.

REFERENCES CITED

Anbu, P., Kang, C.-H., Shin, Y.-J., and So, J. S. (2016). "Formations of calcium carbonate minerals by bacteria and its multiple applications," *SpringerPlus* 5(1), Article number 250. DOI: 10.1186/s40064-016-1869-2

ASTM D143 (2016). "Standard methods of testing small clear specimens of timber," ASTM International, West Conshohocken, PA, USA.

ASTM D2017-81 (1995). "Standard method of accelerated laboratory test of natural decay resistance of woods," ASTM International, West Conshohocken, PA, USA.

ASTM D4442-16 (2016). "Standard test methods for direct moisture content measurement of wood and wood-based materials," ASTM International, West Conshohocken, PA, USA.

ASTM D4446 (1985). "Standard test method for anti-swelling effectiveness of water-repellent formulations and differential swelling of untreated wood when exposed to liquid water environments," ASTM International, West Conshohocken, PA, USA.

ASTM D4933-99 (1999). "Standard guide for moisture conditioning of wood and wood-based materials," ASTM International, West Conshohocken, PA, USA.

Barhoum, A., Rahier, H., Abou-Zaied, R. E., Rehan, M., Dufour, T., Hill, G., and Dufresne, A. (2014). "Effect of cationic and anionic surfactants on the application of calcium carbonate nanoparticles in paper coating," *ACS Appl. Mater. Inter.* 6(4), 2734–2744. DOI: 10.1021/am405278j

Benzerara, K., Miot, J., Morin, G., Ona-Nguema, G., Skouri-Panet, F., and Férard, C. (2011). "Significance, mechanisms and environmental implications of microbial biomineralization," *C. R. Geosci.* 343(2–3), 160-167. DOI: 10.1016/j.crte.2010.09.002

Brown, M., and Gallagher, P. K. (2003). *Handbook of Thermal Analysis and Calorimetry: Vol 2- Applications to Inorganic and Miscellaneous Materials*, Elsevier, Amsterdam, Netherlands. DOI: 10.1016/s1573-4374(03)80002-x

Burgert, I., Keplinger, T., Cabane, E., Merk, V., and Rüggeberg, M. (2016). "Biomaterial wood: Wood-based and bioinspired materials," in: *Secondary Xylem Biology*, Y. S. Kim, R. Funada, and A. P. Singh (eds.), 259-281. DOI: 10.1016/B978-0-12-802185-9.00013-9

Butylina, S., Hyvärinen, M., and Kärki, T. (2012). "Accelerated weathering of wood–polypropylene composites containing minerals," *Compos. Part A-Appl. S.* 43(11), 2087-2094. DOI: 10.1016/j.compositesa.2012.07.003

Cheng, H., Gao, J., Wang, G., Shi, S. Q., Zhang, S., and Cai, L. (2015). "Enhancement of mechanical properties of composites made of calcium carbonate modified bamboo fibers and polypropylene," *Holzforschung* 69(2), 215-221. DOI: 10.1515/hf-2014-0020

Dash, S., Kamruddin, M., Ajikumar, P., Tyagi, A., and Raj, B. (2000). "Nanocrystalline and metastable phase formation in vacuum thermal decomposition of calcium

carbonate," *Thermochim. Acta* 363(1–2), 129-135. DOI: 10.1016/S0040-6031(00)00604-3

Declet, A., Reyes, E., and Suárez, O. M. (2016). "Calcium carbonate precipitation: A review of the carbonate crystallization process and applications in bioinspired composites," *Rev. Adv. Mater. Sci.* 44(1), 87-107.

Dhami, N. K., Reddy, M. S., and Mukherjee, A. (2013). "Biomineralization of calcium carbonates and their engineered applications: A review," *Front. Microbiol.* 4, Article number 314. DOI: 10.3389/fmicb.2013.00314

Dhami, N. K., Reddy, M. S., and Mukherjee, A. (2014). "Synergistic role of bacterial urease and carbonic anhydrase in carbonate mineralization," *Appl. Biochem. Biotech.* 172(5), 2552-2561. DOI: 10.1007/s12010-013-0694-0

Gadd, G. M., Bahri-Esfahani, J., Li, Q., Rhee, Y. J., Wei, Z., Fomina, M., and Liang, X. (2014). "Oxalate production by fungi: Significance in geomycology, biodeterioration and bioremediation," *Fungal Biol. Rev.* 28(2–3), 36-55. DOI: 10.1016/j.fbr.2014.05.001

Gadd, G. M., Rhee, Y. J., Stephenson, K., and Wei, Z. (2012). "Geomycology: Metals, actinides and biominerals," *Env. Microbiol. Rep.* 4(3), 270-296. DOI: 10.1111/j.1758-2229.2011.00283.x

Gaitán-Alvarez, J., Moya, R., Berrocal, A., and Araya, F. (2020). "*In situ* mineralization of calcium carbonate of tropical hardwood species from fast-grown plantations in Costa Rica," *Carbonates and Calcites* (Submited) 2020.

Ganendra, G., De Muynck, W., Ho, A., Arvaniti, E. C., Hosseinkhani, B., Ramos, J. A., Rahier, H., and Boon, N. (2014). "Formate oxidation-driven calcium carbonate precipitation by methylocystis parvus OBBP," *Appl. Env. Microb.* 80(15), 4659–4667. DOI: 10.1128/AEM.01349-14

Hadal, R., Dasari, A., Rohrmann, J., and Misra, R. D. (2004). "Effect of wollastonite and talc on the micromechanisms of tensile deformation in polypropylene composites," *Mater. Sci. Eng.* 372(1–2), 296-315. DOI: 10.1016/j.msea.2004.01.003

Harvie, C. E., Møller, N., and Weare, J. H. (1984). "The prediction of mineral solubilities in natural waters: The Na-K-Mg-Ca-H-Cl-SO_4-OH-HCO_3-CO_3-CO_2-H_2O system to high ionic strengths at 25°C," *Geochim. Cosmochim. Ac.* 48(4), 723-751. DOI: 10.1016/0016-7037(84)90098-X

Hong, K. S., Lee, H. M., Bae, J. S., Ha, M. G., Jin, J. S., Hong, T. E., Kim, J. P., and Jeong, E. D. (2011). "Removal of heavy metal ions by using calcium carbonate extracted from starfish treated by protease and amylase," *Journal of Analytical Science and Technology* 2(2), 75-82. DOI: 10.5355/JAST.2011.75

Hoque, M. E. (2013). "Processing and characterization of cockle shell calcium carbonate ($CaCO_3$) bioceramic for potential application in bone tissue engineering," *J.Material Science & Engineering* 2(4), Article ID 1000132. DOI: 10.4172/2169-0022.1000132

Hübert, T., Unger, B., and Bücker, M. (2010). "Sol–gel derived TiO_2 wood composites," *J. Sol-Gel Science and Technology* 53(2), 384-389. DOI: 10.1007/s10971-009-2107-y

Hull, T. R., Witkowski, A., and Hollingbery, L. (2011). "Fire retardant action of mineral fillers," *Polym. Degrad. Stabil.* 96(8), 1462-1469. DOI: 10.1016/j.polymdegradstab.2011.05.006

Huuhilo, T., Martikka, O., Butylina, S., and Kärki, T. (2010). "Mineral fillers for wood–plastic composites," *Wood Material Science & Engineering* 5(1), 34-40. DOI: 10.1080/17480270903582189

Klaithong, S., Van Opdenbosch, D., Zollfrank, C., and Plank, J. (2013). "Preparation of

$CaCO_3$ and CaO replicas retaining the hierarchical structure of sprucewood," *Z. Naturforsch.* 68(5–6), 533-538. DOI: 10.5560/znb.2013-3062

Krajewska, B. (2018). "Urease-aided calcium carbonate mineralization for engineering applications: A review," *J. Advan. Res.* 13, 59-67. DOI: 10.1016/j.jare.2017.10.009

Kumari, D., Qian, X.-Y., Pan, X., Achal, V., Li, Q., and Gadd, G. M. (2016). "Microbially-induced carbonate precipitation for immobilization of toxic metals," *Adv. Appl. Microbiol.* 94, 79-108. DOI: 10.1016/bs.aambs.2015.12.002

Leong, Y. W., Abu Bakar, M. B., Ishak, Z. A. M., Ariffin, A., and Pukanszky, B. (2004). "Comparison of the mechanical properties and interfacial interactions between talc, kaolin, and calcium carbonate filled polypropylene composites," *J. Appl. Polym. Sci.* 91(5), 3315-3326. DOI: 10.1002/app.13542

Li, Q., Csetenyi, L., and Gadd, G. M. (2014). "Biomineralization of metal carbonates by *Neurospora crassa*," *Environ. Sci. Technol.* 48(24), 14409-14416. DOI: 10.1021/es5042546

Li, Q., Csetenyi, L., Paton, G. I., and Gadd, G. M. (2015). "$CaCO_3$ and $SrCO_3$ bioprecipitation by fungi isolated from calcareous soil," *Environ. Microbiol.* 17(8), 3082-3097. DOI: 10.1111/1462-2920.12954

Liu, C. L. C., Kuchma, O., and Krutovsky, K. V. (2018). "Mixed-species *versus* monocultures in plantation forestry: Development, benefits, ecosystem services and perspectives for the future," *Global Ecology and Conservation* 15, e00419. DOI: 10.1016/j.gecco.2018.e00419

Mantanis, G. I. (2017). "Wood chemical modification," *BioResources* 12(2), 4478-4489. DOI: 10.15376/biores.12.2.4478-4489

Merk, V., Chanana, M., Gaan, S., and Burgert, I. (2016). "Mineralization of wood by calcium carbonate insertion for improved flame retardancy," *Holzforschung* 70(9), 867-876. DOI: 10.1515/hf-2015-0228

Merk, V., Chanana, M., Keplinger, T., Gaan, S., and Burgert, I. (2015). "Hybrid wood materials with improved fire retardance by bio-inspired mineralisation on the nano- and submicron level," *Green Chem.* 17(3), 1423-1428. DOI: 10.1039/C4GC01862A

Moya, R., Salas, C., Berrocal, A., and Valverde, J. C. (2015). "Evaluation of chemical compositions, air-dry, preservation and workability of eight fastgrowing plantation species in Costa Rica," *Madera Bosques* 21, 31-47.

Okwadha, G. D. O., and Li, J. (2010). "Optimum conditions for microbial carbonate precipitation," *Chemosphere* 81(9), 1143-1148. DOI: 10.1016/j.chemosphere.2010.09.066

Ozen, I., Simsek, S., and Eren, F. (2013). "Production and characterization of polyethylene/calcium carbonate composite materials by using calcium carbonate dry and wet coated with different fatty acids," *Polym. Polym. Compos.* 21(3), 183-188. DOI: 10.1177/096739111302100310

Rodriguez-Navarro, C., Jroundi, F., Schiro, M., Ruiz-Agudo, E., and González-Muñoz, M. T. (2012). "Influence of substrate mineralogy on bacterial mineralization of calcium carbonate: Implications for stone conservation.," *Appl. Environ. Microb.* 78(11), 4017-4029. DOI: 10.1128/AEM.07044-11

Sãnchez-Romãn, M., Rivadeneyra, M. A., Vasconcelos, C., and McKenzie, J. A. (2007). "Biomineralization of carbonate and phosphate by moderately halophilic bacteria," *FEMS Microbiol. Ecol.* 61(2), 273-284. DOI: 10.1111/j.1574-6941.2007.00336.x

Shabir Mahr, M., Hübert, T., Sabel, M., Schartel, B., Bahr, H., and Militz, H. (2012). "Fire retardancy of sol–gel derived titania wood-inorganic composites," *J. Mater. Sci.*

47(19), 6849-6861. DOI: 10.1007/s10853-012-6628-3

Singh, N. B., and Singh, N. P. (2007). "Formation of CaO from thermal decomposition of calcium carbonate in the presence of carboxylic acids," *J. Therm. Anal. Calorim.* 89(1), 159-162. DOI: 10.1007/s10973-006-7565-7

Stark, N. M., and Gardner, D. J. (2008). "*Outdoor durability of wood–polymer composites*," in: Wood–Polymer Composites, Woodhead Publishing, Ltd., Cambridge, England, pp. 142-165. DOI: 10.1533/9781845694579.142

Steenkjær Hastrup, A. C., Jensen, B., Clausen, C., and Green, III, F. (2006). "The effect of $CaCl_2$ on growth rate, wood decay and oxalic acid accumulation in *Serpula lacrymans* and related brown-rot fungi," *Holzforschung* 60(3), 339-345. DOI: 10.1515/HF.2006.054

Sun, S., Li, C., Zhang, L., Du, H., and Burnell-Gray, J. (2006). "Interfacial structures and mechanical properties of PVC composites reinforced by $CaCO_3$ with different particle sizes and surface treatments," *Polym. Int.* 55(2), 158-164. DOI: 10.1002/pi.1932

Taghiyari, H. R. (2012). "Fire-retarding properties of nano-silver in solid woods," *Wood Sci. Technol.* 46(5), 939-952. DOI: 10.1007/s00226-011-0455-6

Tampieri, A., Sprio, S., Ruffini, A., Celotti, G., Lesci, I. G., and Roveri, N. (2009). "From wood to bone: Multi-step process to convert wood hierarchical structures into biomimetic hydroxyapatite scaffolds for bone tissue engineering," *J. Mater. Chem.* 19(28), 49-73. DOI: 10.1039/b900333a

Tenorio, C., Moya, R., Salas, C., and Berrocal, A. (2016). "Evaluation of wood properties from six native species of forest plantations in Costa Rica," *Bosque* 37(1), 71-84. DOI: 10.4067/S0717-92002016000100008

Tourney, J., and Ngwenya, B. T. (2009). "Bacterial extracellular polymeric substances (EPS) mediate $CaCO_3$ morphology and polymorphism," *Chem. Geol.* 262(3–4), 138-146. DOI: 10.1016/j.chemgeo.2009.01.006

Tsioptsias, C., and Panayiotou, C. (2011). "Thermal stability and hydrophobicity enhancement of wood through impregnation with aqueous solutions and supercritical carbon dioxide," *J. Mater. Sci.* 46(16), 5406-5411. DOI: 10.1007/s10853-011-5480-1

Uribe, B. E. B., and Ayala, O. A. (2015). "Characterization of three wood species (Oak, Teak and Chanul) before and after heat treatment," *Journal of the Indian Academy of Wood Science* 12(1), 54-62. DOI: 10.1007/s13196-015-0144-4

Walters, R. N., and Lyon, R. E. (2003). "Molar group contributions to polymer flammability," *J. Appl. Polym. Sci.* 87(3), 548-563. DOI: 10.1002/app.11466

Wu, Y., Zhao, C., Jiang, Y., and Han, W. (2016). "Study on modification of calcium carbonate for paper filler," in: *Proceedings of the 2016 4th International Conference on Machinery, Materials and Computing Technology*, Atlantis Press, Paris, France, pp. 395-398. DOI: 10.2991/icmmct-16.2016.80

Yao, F., Wu, Q., Lei, Y., Guo, W., and Xu, Y. (2008). "Thermal decomposition kinetics of natural fibers: Activation energy with dynamic thermogravimetric analysis," *Polym. Degrad. Stabil.* 93(1), 90-98. DOI: 10.1016/j.polymdegradstab.2007.10.012

Zeng, Y., Cao, J., Wang, Z., Guo, J., Zhou, Q., and Lu, J. (2018). "Insights into the confined crystallization in microfluidics of amorphous calcium carbonate," *Cryst. Growth. Des.* 18(11), 6538-6546. DOI: 10.1021/acs.cgd.8b00675

Article submitted: Jan. 27, 2020; Peer review completed: April 25, 2020; Revised version received: April 29, 2020; Accepted: April 30, 2020; Published: May 7, 2020.
DOI: 10.15376/biores.15.3.4802-4822